Thermal Runaway: Can Ultrasound Finally Solve Li-ion Cells' Most Dangerous Challenge?

熱暴走：超音波はリチウムイオンセルの最も危険な課題を解決できるか？

Michele BRAGLIA
ミシェル ブラグリア

Richard STOCKER
リチャード ストッカー

The occurrence of several battery-related accidents over the years has risen public awareness of risks and safety issues around electric vehicles (EVs). Current safety features implemented on battery management systems (BMSs) heavily depend on thermocouples instrumented to the surface of the cell. However, for an effective early warning system, the ability to record or detect internal changes of a cell is vital. One technique that may be ideally suited to this is ultrasonic measurement. As part of a European Automobile Manufacturers' Association (ACEA)-funded project, HORIBA MIRA has been collaborating with University College of London (UCL) to explore the use of ultrasound to detect internal changes in a cell to pre-emptively warn about thermal runaway (TR). This article reports on experimental studies aimed at evaluating the application of ultrasonic sensors to detect abuse conditions and early TR signals in battery cells. The changes in acoustic behaviours of battery cells have been monitored and evaluated during temperature-controlled, nail penetration, and overcharge as well as homogeneous and localised heating tests. Finally, ultrasound's ability to capture key events during thermal runaway propagation scenarios has been assessed by triggering TR in a cell of a small prototype module.

近年，バッテリーに関連する事故が頻発し，電気自動車(EV)のリスクと安全性に対する社会的な認識が高まっている。バッテリー管理システム(BMS)に搭載されている安全機能は，セル表面に取り付けられた熱電対に大きく依存している。しかし，効果的な早期警告システムのためにはバッテリーの内部変化を記録・検出する能力が不可欠であり，そのために最適な技術の一つが超音波測定である。欧州自動車工業会(ACEA)が資金提供するプロジェクトの一環として，HORIBA MIRAはロンドン大学(UCL)と共同で，熱暴走(TR)を事前に警告するためにセルの内部変化を検出する超音波の利用法を研究している。本稿では，バッテリーセル内部の異常状態の検出や熱暴走の兆候の早期検出のために超音波センサーを応用した実験研究を報告する。

Introduction

In lithium-ion batteries (LIBs), accidents stem from two broad issues. In the first type, a cell or a battery pack can fail due to mechanical, thermal, or electrical abuse. During mechanical abuse, the two electrodes connect due to nail penetration, fracture of the separator, or deformation of the electrode. When the battery is subject to electrical abuse, such as over-discharge, metallic dendrites (mainly lithium or copper) grow on the anode surface and may penetrate the separator. Thermal abuse occurs when the cells are cycled/stored at excessive temperature, triggering the thermal decomposition of the materials inside the cells.

The second type of safety accident is generally the most feared since it occurs during the seemingly normal operations of the battery. These faults give no clear warning signals and are the most difficult to predict and detect. Such accidents are often due to the presence of internal short circuits (ISCs) caused by foreign metal particles that contaminate the electrode materials during the manufacturing process. These contaminants, in electrochemical contact with the cathode, are oxidized and dissolved into the electrolyte during cycling. They then diffuse and plate on the anode, piercing the separator and causing an ISC (grown-in internal shorts). When a large area ISC is formed, the electric energy is released at a high rate in

that area, rapidly increasing the internal temperature and, possibly, triggering TR. ISC has been the main cause of recalls of automotive LIBs.[1] This class of safety accidents is particularly eared as safety components incorporated in today's lithium-ion cells and battery packs are not effective.

What is Thermal Runaway and Why it is Challenging to Avoid

Both classes of safety accidents can trigger TR. During thermal runaway (Figure 1) the cell temperature increases due to exothermic reactions. In turn, the increased temperature accelerates the decomposition reactions and the system quickly destabilizes. At the end of the TR, temperatures higher than 1000 °C can be reached and high amounts of flammable and harmful gases are released.[2]

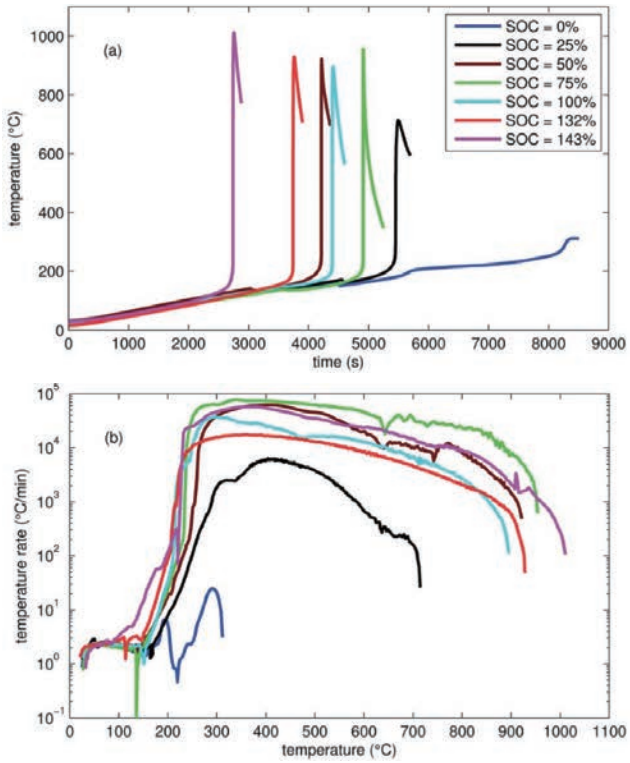

Figure 1 TR induced by thermal ramp experiments on NCA cathode cells at different states of charge.
(a) Cell temperature profiles, (b) Cell temperature rate vs. cell temperature. Adapted from.[2]

If a cell fails in a battery pack it can lead the surrounding cells to also fail, causing a chain reaction within the pack with potentially serious consequences which is known as thermal runaway propagation (TRP). Such an event is particularly scary in the automotive industry where high-capacity cells present in battery pack modules are often spaced less than 1 mm and, in some cases, there might even be direct contact among adjacent cells. In modules with banks of cells in parallel, if one cell experiences an ISC it can act as a short for the entire bank, leading to an external short for the remaining cells.

The BMS is a key safety component of the battery pack as, if properly designed, it can keep the battery pack from operating in unsafe conditions. However, some relevant issues arise when considering its implementation on EV battery packs. Standard BMSs rely on temperature readings from thermocouples located on the surface of the cell which, in the case of large cells, can be very different from the temperature of their centre. The formation of an internal cell temperature gradient can create local gassing and accelerated cell degradation. The cooling system, regardless of its efficiency, has limited efficacy on temperature gradients as it can only cool the cell surface. If not properly considered by the BMS, ageing can also cause cell unbalance which can limit cell capacity, accelerate degradation, or cause electrical abuse of some of the cells. The number of safety-related accidents that have occurred recently indicates that in some cases current BMSs alone can be inadequate.[3][4] For an effective early warning system, the ability to detect internal temperature changes is vital.

Legislation

On the 12th of May 2020, China issued three mandatory standards for EVs safety that relate to the EV battery, the EV itself and electric buses. The battery regulations mandate improved battery system safety regarding thermal diffusion, external fire, mechanical shock, simulated collision, thermal and humidity cycling, external short circuit, overcharge, and over-temperature. In addition, in the case of TR of one cell, no fire or explosion should occur in the cabin for at least 5 minutes, allowing for occupants to escape the vehicle. The battery system is required to notify the vehicle occupants of a thermal incident immediately. More stringent requirements for preventing water ingress, ensuring proper insulation and battery monitoring are also included. Due to their larger battery packs, the new standards for electric buses have more rigorous demands on battery casing collision, charging and water ingress. The standards request for appraisal of the flame-retardant performance, TR prevention and the battery management unit.[5]

To date, there exists a wide variety of battery designs and thermal management strategies across the various EVs. Manufacturers have varied between cylindrical, pouch and prismatic cells with air, water-glycol, or refrigerant-based cooling. As regulations like these are enforced it may well push the industry towards one solution. Emerging technologies like immersion cooling, where the cells are immersed in a flame-retardant dielectric fluid,

may start to take a larger share of the market. Detecting thermal events in vehicles is also a widely unexplored area of the market. Another consideration is how to notify passengers and if an active method of extinguishing the battery pack should be incorporated into the design. Crucially, all the methods have their limitations and it is imperative to avoid false positives and potentially extinguish a battery that is working correctly, as this is often the most expensive component in the vehicle.[5]

Factors of Risk

In current LIBs the cathode chemistry plays a major role with regard to proneness to TR. Transition metal oxides commonly employed as a cathode in LIBs become structurally unstable if their thermal decomposition temperature (TR onset temperature) is reached. The consequent release of the oxygen present in their crystalline structure prompts the combustion of the liquid electrolyte sustaining a rising heating rate that leads the cell to irreversibly enter TR. Among the commercially employed cathode materials, lithium iron phosphate (LFP) presents highest thermal stability. Nickel manganese cobalt oxide 111 (NMC111), has slightly better thermal stability than nickel cobalt aluminium oxide (NCA), which, combined with its good energy density, makes it one of the most widespread cathode materials in current LIBs. The thermal decomposition with associated oxygen release occurs at around 350 °C for LFP, 280 °C for NCA and 300 °C for NMC 111. The thermal stability of the high Ni-content cathodes as NMC 811 drastically decreases, with thermal decomposition starting already at 150 °C in the case of the NMC 811.[6]

The thermal stability of carbonaceous and transition metal oxides is a function of the state of charge (SoC). This becomes particularly evident in the case of overcharge where TR onset temperatures decrease sharply as SoC increases. The onset temperatures of thermal decomposition in overcharged NCA cells can go as low as 65 °C.[6]

Cell design is also crucial for safety. Nanomaterial- level design strategies can allow the usage of thermally unstable materials (Ni-core rich, Mn-shell rich active materials). A crucial design parameter for safety is the capacity load ratio. The anode should be present in slight excess with respect to the cathode to avoid lithium plating due to loss of anode active material during ageing. Kinetics mismatch between anode and cathode must also be avoided and the porosity of the electrodes must be properly implemented.

The geometry of the cell also has some important consequences on safety. Pouch cells are sometimes considered safer since they can freely expand and release pressure. However, safety vents are installed on rigid prismatic and cylindrical cells. The design and size of the vent are critical to ensure suitable pressure management. An important parameter is also the cell size. Larger cells contain more chemical energy, exhibit higher temperature gradients and their cooling is less effective due to the lower surface-to-volume ratio.

Experimental TRP studies have shown that cell spacing, tab connection, vents location/design and thermal barriers are the key parameters to mitigate TRP risks. However, the empirical nature of such tests makes their validity limited to the specific assembly and configuration tested. Small differences in cell designs, cell manufacturing methods and ageing states can severely affect the results of such tests.

Methods to Monitor Battery Packs

Optimal combinations of cell materials, design and advanced BMS strategies can reduce but not eradicate the risk of TR. Thus, it is crucial to develop methods that can promptly detect nascent TR to give the BMS more time to take suitable countermeasures or to passengers to leave the vehicle. Some TR detection methods are presented and schematically illustrated in Table 1:

- Gas/pressure/strain gauge sensors: gas generation starts occurring in the very early stages of TR, regardless of the cell type, chemistry, and format. During overheating, the liquid electrolyte expands, the internal pressure increases, and the gas is vented out of the cell. Gas and pressure sensors were proven to be capable to detect TR onset more quickly than non-embedded temperature sensors and in a stage in which TR can still be impeded if suitable countermeasures are adopted.[9] Each sensor type has its characteristic detection speed, signal clarity and actual deployment feasibility. A combination of different sensors could be instrumented to a cell to correlate each measured signal with the TR onset and the best sensors setup to detect TR identified.
- Other techniques based on self-discharge current detection, cell modelling (equivalent circuits, Kalman filters), consistency analysis of parameters within the battery pack and electrochemical impedance spectroscopy have been successfully implemented and applied to detect ISC or thermal abuse and have good potential to be implemented onboard.[10]-[20]

Table 1 Matrix summarising the TR detection methods listed in this document and their relative pros and cons.

·Detection methods	Advantages	Disadvantages
·Self-discharge measurement	- Simple, quick, and effective in detecting ISC	- Conventional methods to measure self-discharge are time-intensive (typically taking days or even weeks), costly, complex and/or not well-difined - TR triggered by thermal, mechanical, and electrical abuse is not directly detected
·Consistency within the battery pack	- Cheap and easy to implement onboard	- Relies on external temperature readings - Threshold for deviations from normal conditions might cause unacceptably frequent stops and too loose conditions might be ineffective in timely detecting TR
·Multi-sensors	- A suitable combination of different types of sensors can provide an early warning of TR	- Temperature and voltage sensors are not effective to detect TR under certain conditions. Their combination with other sensors increases system cost and complexity - More prone to sensor failure - The interpretation of the sensore's readings might not be so straightforward and false alarms can be generated since gas and pressure increases can occur also during normal battery operation
·Internal short circuit modelling	- Does not require additional sensors onboard (only I, V and T sensors needed)	- Complexity, computational resources - Can be hard to verify/adapt to different cell types
·Impedance spectroscopy	- Can infer the internal temperature of a cell - In the case of certain I, V input signals (i.e. square waves) it can be applied onboard	- Its adaptation and interpretation for different cell chemistries might be cumbersome since the SoC and the ageing of the battery can be difficult to separate from the temperature effect

A Novel Approach: Acoustic Impedance

Ultrasonic testing is a non-destructive technique based on monitoring how ultrasound waves propagate through an object of interest. In industry, ultrasound is typically used to test for cracks within materials, measure thicknesses and monitor corrosion of pipes. Another common use is in underwater range finding (Sonar) in which by measuring the difference in time between the pulse being transmitted and the echo being received, it is possible to determine the distance of an object. In medical imaging, ultrasound is used to visualize muscles, tendons, and many internal organs to capture their size, structure and any pathological lesion with real-time tomographic images. The technology is relatively inexpensive and portable, especially when compared with other techniques, such as magnetic resonance imaging and computed tomography. Recently, ultrasound is gaining attention for the study of electrochemical devices.[21]-[23] The main advantages of this technique are that it is non- destructive, can be conducted operando, it is relatively cheap, and measurements are very quick, taking only microseconds to complete.

Working Principle and Potential for Monitoring Batteries Safety

In the battery test bench used for acoustic analysis, a cell equipped with an ultrasonic transducer and a thermocouple is placed inside a thermal chamber and connected to an external battery cycler and an ultrasonic multiplexer which generates and record the electrical and acoustic signals. When conducting an ultrasonic measurement, a very short ultrasonic pulse wave is generated by a piezoelectric transducer. The signal then travels through the object of interest and the wavefront is a influenced by the properties of the object's component materials. The signal is then either received by a second transducer on the other side of the object (Transmission) or the reflected waves are received by the same transducer that generated them (Pulse Echo). An important acoustic wave property is the time of flight (ToF) which is the time taken for the generated wave to travel through the object and is affected by the speed of sound through the material through which it propagates.

Typical waveforms obtained for pulse-echo mode and transmission set-ups performed on the same cell are shown in Figure 2.[30] In pulse-echo mode Figure 2a, the initial signal at a ToF below 1 µs is due to the generation of the initial ultrasonic pulse and is not influenced by the cell under study. The peaks at ToF values higher than 1 µs are reflection peaks related to the internal structure and the interfaces present within the cell. Acoustic peaks corresponding to higher ToFs reflect the properties of interfaces located farther from the acoustic emitting device. The amplitude of these internal reflection peaks decreases steadily with penetration depth due to signal attenuation and reflection in previous layers. At ca 8.7 µs a peak with a slightly higher amplitude is observed. This is referred to as the first echo peak and corresponds to the part of the ultrasonic signal that has travelled all the way through the cell and hit the back case. Due to the large difference in acoustic impedance between the cell and the external air, nearly all the signal is reflected resulting in the slightly higher amplitude observed. In the transmission set-up (Figure 2b) a strong peak is observed at a ToF approximately half of that observed for the pulse-echo experiments. The strong multiple peaks observed at lower ToFs in pulse-echo mode are no longer observed as these are due to reflections from the internal layers within the cell.

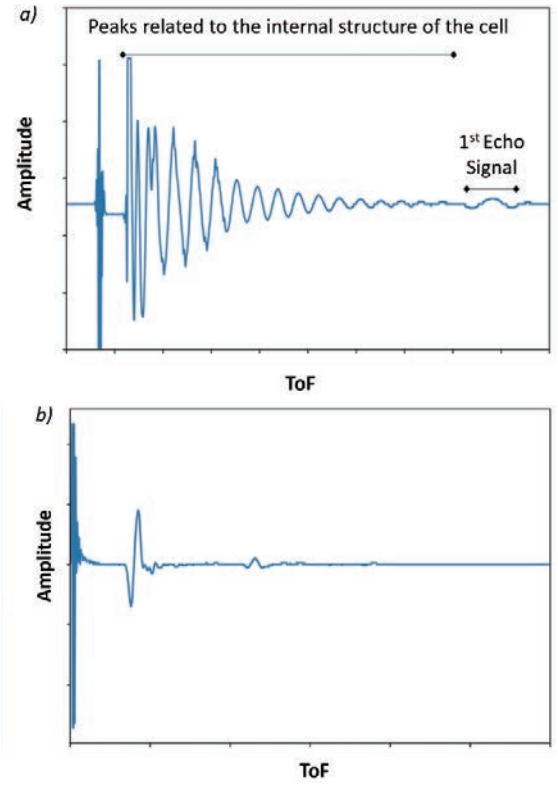

Figure 2 Typical acoustic waveform generated from a) pulse- echo mode and b) transmission mode setups. Adapted from.[30]

LIBs present a typical layered structure in which the anode is constructed of a carbon material supported on a copper current collector, the cathode consists of an active material, typically a metal oxide such as NCA or NMC supported on an aluminium current collector, and a separator which ensures that no direct contact is made between the anode and the cathode. Such layers are then wrapped together to form the so-called jelly roll. All components in the pouch cell are soaked in an electrolyte solution which acts as an acoustic couplant between different layers and allows the acoustic signal to travel through the cell. When an ultrasound waveform is generated by the transducer placed on the surface of the cell, the wavefront travels through the cell. At every material interface, some of the signal is transmitted and some is reflected back towards the transducer. The percentage reflected and transmitted is dependent on the difference between the acoustic impedance of the two materials. As the material properties change with cycling, the speed of sound through the materials will also be affected resulting in a shift in peak's ToFs. In addition, the electrode layers expand and contract as lithium ions move, also resulting in shifts in peak's ToFs.

The capability of acoustic waves to unveil information about internal interfaces and material properties of batteries has recently led to initial studies in which ultrasound and acoustic sensors have been employed to estimate SoC and state of health (SoH),[22]-[27] but only few have reported the use of acoustic measurements to monitor abuse testing of LIBs.[28] For the interested reader, the experimental studies here reported have been published in specialised scientific journals.[29][30]

Experimental Work Between HORIBA MIRA and UCL

This study aimed to assess the practical capability of acoustic-based techniques to promptly inform about abusive operating conditions occurring within battery cells. It explored the method's potential to be effectively employed in real-world applications as an early TR detection method, benchmarking it against currently employed sensors such as thermocouples and voltage sensors. A broad range of techniques for inducing TR (including nail penetration, overcharge as well as uniform and localised heating) was tested on several 210 mAh pouch cells based on a lithium cobalt oxide cathode (LCO) and a graphite anode. The acoustic measurements were compared with voltage and temperature readings and X-ray radiography was employed to give further physical insight and support findings from acoustic measurements. The TRP through a small module of cells was investigated with the use of multiple transducers.

Results

Internal Temperature

To determine how the temperature of the cell affects the waveform generated by ultrasonic analysis, a 210 mAh pouch cell was set up in an environmental chamber and the acoustic signal was monitored as the temperature was varied.[30] Figure 3a shows a plot of how the temperature was altered with time . To investigate the cell behaviour in mildly abusive conditions, the temperature was varied beyond the window temperature assigned by cell manufacturers (0-40 °C). A colourmap plot of how the acoustic signal changes during this period is shown in Figure 4b. This plot is effectively a top-down view of how the typical signal varies with temperature. Each line shows a peak, with the colour indicating the amplitude and its position in the y-direction indicating the ToF.

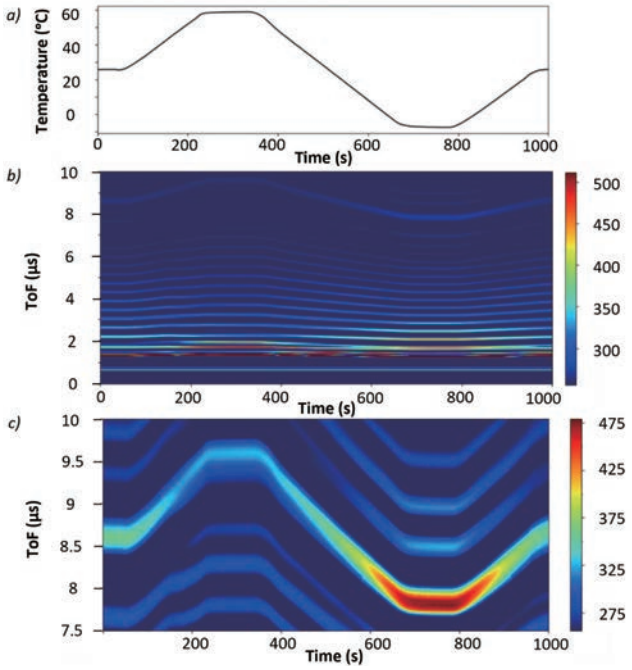

Figure 3 (a) A plot of how cell temperature varied over the course of the experiment. (b) A colourmap plot showing how the received acoustic waveform varied over the course of the temperature experiment. (c) A colourmap plot of how the first echo peak varies as the temperature is varied over the duration of the experiment. Adapted from.[30]

As the temperature is initially held constant, no variation in amplitude or ToF is observed with any peak. During heating the ToF of each peak increased due to the individual anode and cathode layers expansion, causing the entire cell to swell accordingly. The effect becomes more pronounced as the ToF of the peak increases since for reflections from deeper interfaces the signal must travel farther through the changing battery materials and the effects are increased. As the cell is cooled the changes are reversed due to the contracting of the cell, while the amplitude of all peaks increases. The first echo peak, located at 8.75 µs, shows the largest shift in ToF with temperature.

For the temperature to be accurately predicted using the acoustic techniques, an understanding of how the SoC of the cell affects the relationship is required. To investigate this, the previous experiment was repeated at various SoCs and the results are summarised in Figure 4.[30] For all SoCs, a linear relationship between the first echo peak's ToF and the temperature is observed, with a similar gradient between 0 and 50 °C, which allows to easily measure the internal temperature of a given cell. At higher and lower temperatures, the correlation deviates from linearity suggesting cell ageing/damage. This damage is likely due to taking the cell outside of the manufacturer's temperature specifications. Small deviations from the predicted linear relationship between ToF and temperature could then be used to detect and measure the extent of cell damage. This may represent a powerful tool for predicting the onset of irreversible cell degradation and TR.

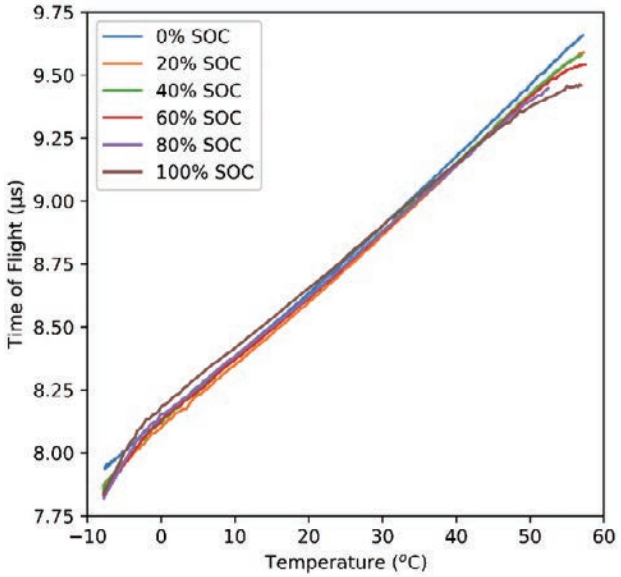

Figure 4 The variation of ToF of the first echo peak at various SOCs. Adapted from.[30]

For the applicability of ultrasound in automotive, the technique must apply to a wide range of cell geometries and capacities. As a proof of concept to show the flexibility of the technique, a range of cell geometries and capacities from a range of manufacturers were also tested. Tests on a 400 mAh cell with same cell chemistry and construction techniques from the same manufacturer and on a 20 Ah A123 pouch cell using both through-transmission and pulse-echo experiments gave consistent results with higher ToFs than the 210 mAh cell as would be expected.

The effect of the cell geometry was also explored via cylindrical cell testing in pulse-echo and transmission mode. Pulse-echo measurements did not prove successful with no repeatable readings obtained whereas tests in transmission mode did prove successful. Transducers were set up at 180º configuration. It was also found that if the transmit and receive transducers are not aligned (180º set-up) and instead are placed with a slight angle between them, the obtained results vary. The propagation of lamb waves around the outer can of the cylindrical cell results in two additional wavelets that appear in the waveform. Depending on the angle of the receiver transducer relative to the transmission transducer the ToF of these lamb waves is altered. This feature shows the potential to detect can swelling as well as surface defect formation by monitoring how the two lamb waves behave.[29]

Detection of Internal Defects

To determine the ability of acoustics to detect any defects that may be present in cells or formed during operation/abuse, acoustic tests were run on two 400 mAh pouch. One of the cells was unused whereas the other had been cycled multiple times during which a sudden failure had occurred. Typical waveforms obtained from transmission experiments for both the 'good' and 'defective' cell are shown in Figure 5.[29]

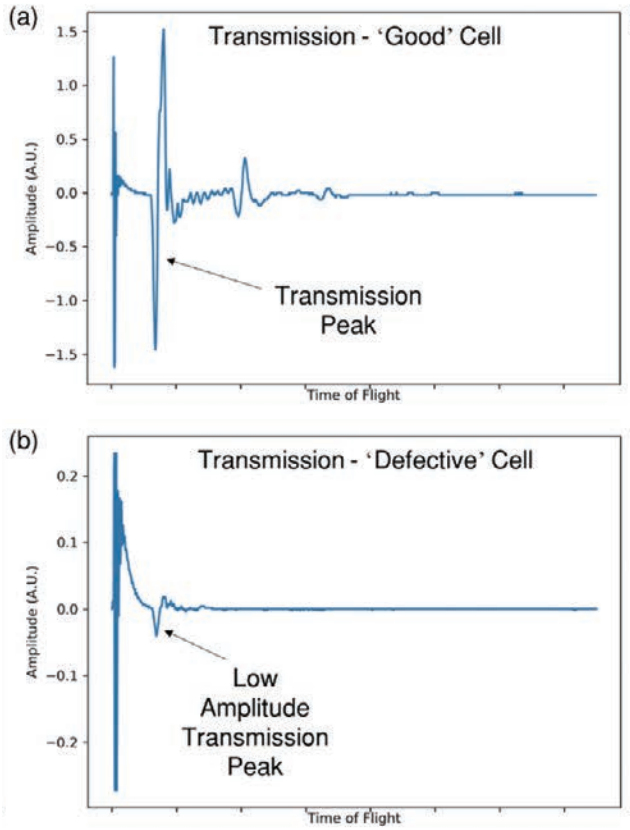

Figure 5 The difference in transmission results for a 'good' 400 mAh cell (a) and a 'defective' cell (b). Adapted from.[29]

The 'good' cell shows a high amplitude transmission peak (Figure 5a) whereas the 'defective' cell also shows the transmission peak at the same ToF but the amplitude has dropped significantly. These results suggest the presence of a defect since the formation of any gases or defect would inhibit good acoustic contact between the electrode layers. To investigate this, the defective cell was studied using X-ray computed tomography.[29] Figure 6 shows visible layer separation at 160 µm. These tests show that even small defects can lead to significant changes in the acoustic signal.

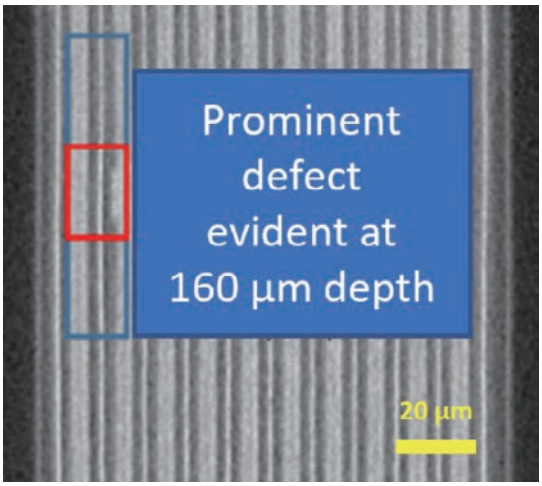

Figure 6 X-ray computed tomography results showing the internal structure of the 'defective' 400 mAh cell shows the prominent defect.. Adapted from.[29]

Thermal Runaway Studies at Cell Level

To acoustically monitor TR in individual cells and its propagation through a module or pack consisting of multiple cells, a method for triggering TR which is reliable, repeatable, and representative of EVs in real- world applications is required. Several methods were tested with a focus on those that would most closely replicate a TR event triggered by an ISC.

The first method tested was nail penetration. Nail penetration is generally regarded as the industry standard test for replication of ISCs. For internal shorts, the highest rates of reaction and largest temperature increases are expected to occur around the nail. Thus, the surface temperature of the cell is not representative of the higher temperatures within the cell. To assess the ability of ultrasound to measure the extent of damage that occurs during TR, several tests were conducted with the chosen cell, a 210 mAh LCO pouch cell, at various SoCs under the assumption that a higher SoC would release more energy during failure and cause more damage. The results showed a sudden loss of acoustic signal in all tests regardless of the SoC of the cell or the amount of damage induced, proving its high sensitivity to the structural damage caused by a nail penetration in the cell.

Another method for inducing TR is by overcharge. Overcharge of LIBs in constant current mode can lead to rapid temperature increase and eventually induce TR. For these tests, C-rates significantly above those recommended by the manufacturer's specification were chosen. A fully charged cell (4.2 V) was overcharged at 10 C followed by 20 C while acoustic measurements were conducted. A strong influence on the acoustic signal was observed. However, the complex nature of the processes occurring within the cell made this technique unsuitable as a method of triggering TR. The overcharge tests did

however suggest that the acoustic methodology could be useful for understanding the process occurring within the cell during overcharge.

Thermally-induced TR, i.e. TR triggered by heating the cell until it fails, is one of the simplest methods for inducing cell failure. To study the ability of acoustic sensors to monitor thermally-induced TR, a cell with a transducer attached was heated between two heating plates. While repeatable and consistent acoustic signals were observed for cells operating under normal conditions, when the cells were pushed outside these limits toward dangerous temperatures, clear changes in acoustic signals were visible. At lower temperatures, additional peaks were observed indicating the presence of additional interfaces within the cell as thermal damage occurs. When the temperature increased further, the ToF of the first echo peak shifted quite drastically before disappearing completely at ca. 100 °C, when the electrolyte likely evaporated. Importantly all these distinct and measurable changes occurred long before the cell entered irreversible TR.

Thermally-induced TR was proved to be a useful method for inducing TR. However, homogeneous heating of the cell is less representative of the type of thermal abuse that would likely occur in a real-world application caused by an ISC, where higher thermal gradients would be more localised within the cell. To make the tests more representative, a heating cartridge was used to heat a small area of the cell to represent the area where a short is occurring. A fully charged cell was heated from the bottom of the cell with a heating cartridge, while an acoustic transducer was placed on the top of the cell. The results of the experiment showed that the voltage remained relatively consistent until the cell entered TR, proving that monitoring cell voltage does not reveal damaging processes occurring within the cell. Over the first 150 seconds, while there was little to no change observed in the temperature recorded by the thermocouple placed on the top of the cell by the transducer, significant changes in the acoustic signal were observed. The echo peak (close to the heating cartridge) was the first peak to disappear, followed sequentially by peaks at lower ToFs, about 500 seconds before the cell entered TR. Importantly, readings from the thermocouples only showed a mild temperature rise throughout.

Thermal Runaway Propagation at Module Level

For higher power operations battery modules or packs are often used, in which multiple cells are connected in series to provide higher voltages and in parallel to provide higher currents (Figure 7).

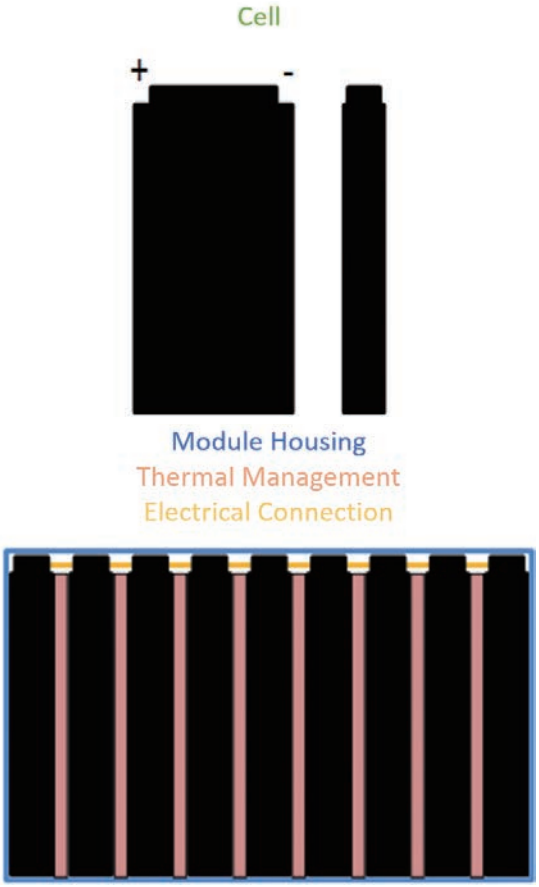

Figure 7 Single-cell and multiple cells assembled in the module configuration.

Understanding the operation of these packs and the inherent risks is of vital importance. Failure of a single cell can easily trigger the rapid heating and consequential failure of neighbouring cells causing a thermal propagation chain reaction.

To study the effectiveness of the ultrasonic technique in pack applications, a small four-cell demonstration module was constructed. Each of the four cells was placed side by side and connected in parallel with a transducer placed on the surface of each of the cells. Thermocouples were placed on the top and bottom of each cell to monitor the temperature of each cell and the thermal gradient from the top of the cell to the bottom.

To determine the expected variation in acoustic signal during normal operation the pack was first left at rest or 15 min before being discharged at 1 C, then immediately charged again at 1 C. All cells exhibited similar acoustic signatures, with changes in the acoustic signals which were measurable but not significant compared to the changes observed in the TR tests.

The four-cell module was then subjected to an abuse test (Figure 8). A heating cartridge was placed on the underside of Cell 4 to trigger localised damage followed by TR. Initially, all cells were held at room temperature for ca.

400 seconds. Then, the heating cartridge in contact with the base of Cell 4 was switched on. All cells were supported on a heat-proof mat with the heating cartridge only in contact with Cell 4. The results from this test are summarised in Figure 9, with the acoustic behaviour of the cells shown along with the temperature of the bottom of each cell.

During rest at room temperature, no shift in any of the acoustic signals is observed. As soon as the localised heating on Cell 4 is initiated, the acoustic signal of this cell begins to change. For clarity, the change in ToF of the first echo peak has been plotted for all cells in Figure 10 and compared to the temperature of the top and bottom of the cell. During heating, the ToF of the first echo peak of Cell 4 rapidly increases beyond any change that would be expected under normal operation.

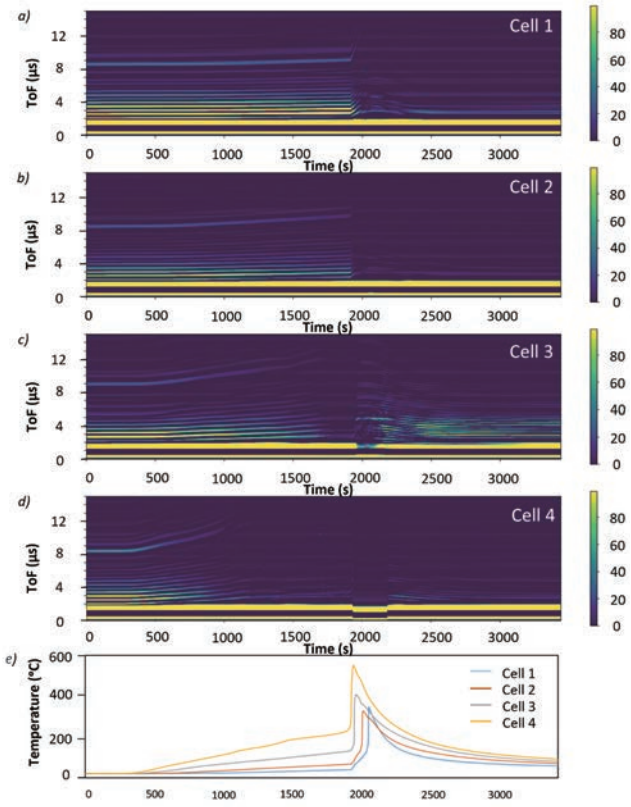

Figure 8 The propagation of thermal failure through a four-cell pack. The acoustic behaviour of Cell 1 (a), Cell 2 (b), Cell 3 (c) and the thermally abused Cell 4 (d) are shown as well as the temperature of the bottom of each cell (e).

After ca. 1000 seconds, the peak amplitude drops and the signal is lost. Meanwhile, the top of the cell is at 70 °C and the bottom at 117 °C, sufficient for electrolyte evaporation. At this point, the acoustic signal has indicated that a significant thermal event and/or damage has occurred to Cell 4. The cell, however, is heated for a further 900 seconds (15 minutes) before it enters TR. The ToF of the first echo peak in Cell 3 also begins to shift as soon as the heating of Cell 4 begins, albeit at a slower rate. After 1400 seconds, 400 seconds slower than Cell 4, the amplitude of the first echo peak in Cell 3 is also lost. The temperature at the bottom of the cell is ca. 100 °C at this point. As Cell 4 enters TR, the heat produced also causes Cell 3 to rapidly heat and enter TR. Cell 2 and Cell 1 also follow similar dynamics although at slower rates due to their farther location from the cell that first undergoes TR. However, the ToF of the first echo peak remains visible until the cells enter TR, suggesting they were still relatively undamaged until the flames coming from the other cells reached them.

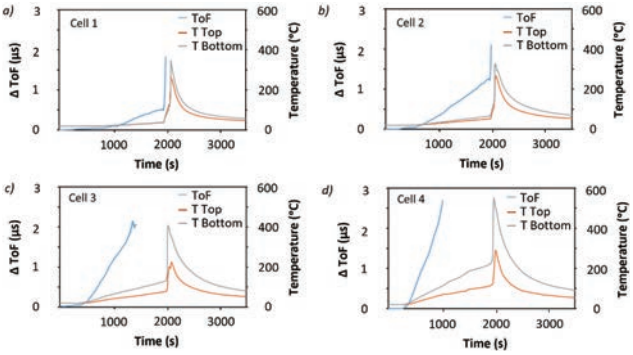

Figure 9 The temperature and ToF variation of the module cells (a) Cell 1, (b) Cell 2, (c) Cell3, (d) Cell 4.

Since the change in ToF of the first echo peak can be both measured using acoustics and predicted based on thermocouple measurements, a potential method to detect unexpected heating or damage is to look for any changes in ToF that are unexpected based on thermocouple readings. To explore this, the ToF of the first echo peak was tracked and the predicted ToF change calculated based on a thermocouple measurement. The predicted value was then subtracted from the measured one. When the cell was operated in normal conditions a value of zero was returned. Conversely, when any change in temperature that wasn't measured by the thermocouple occurred, the predicted and measured values differed, resulting in a deviation from zero. This deviation indicated that a temperature shift not recorded by the top thermocouple was occurring. This type of measurement seems promising to detect any internal temperature changes, such as those caused by ISCs.

Repeatability and Susceptibility to False Positives

For this technology to be implemented in a BMS, the measurements must be robust, repeatable, and not susceptible to false positives. While more work needs to be done before the acoustic temperature measurement technique can be employed commercially, initial results are promising. All tests reported in this study show consistent results with similar acoustic behaviours observed in all TR experiments. The acoustic waveform observed is consistent from cell to cell and the changes observed during

failure are significantly larger than any changes observed in normal use, as shown in Figure 10. The cell to cell variation under normal operation (cycling at the cell's max C rate) is significantly smaller than the changes observed for all cells in the module tested. The point at which each cell reached 60 °C, the cell's maximum working temperature, is also marked on the plot and demonstrates that, based on acoustic readings, an indication of an issue with each cell would have been recorded long before the cell entered an irreversible self-heating process or TR.

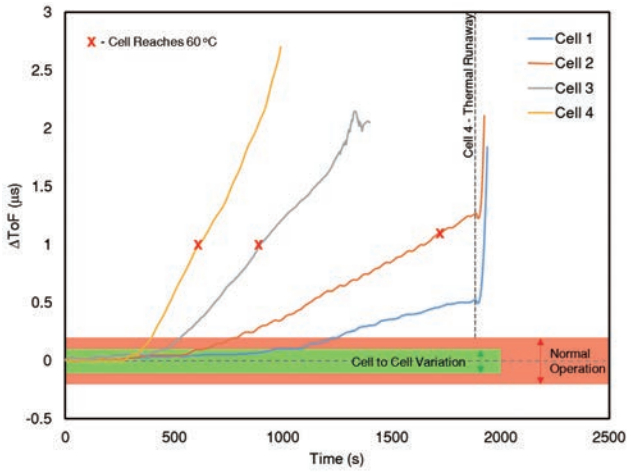

Figure 10 The changes in ToF for each peak relative to cell-to- cell variation and changes in ToF during regular operation.

Conclusions and Further Research

This study demonstrated the ability of ultrasound measurements to accurately monitor the internal temperature of a cell, detect rapid heating and indicate when a cell is about to enter TR well before conventional methods based on voltage and temperature readings. In the module setup, the acoustic signature of the first echo pulse is lost is ca. 900 seconds before the cell enters TR. It was shown that ultrasonic testing can be used to probe virtually all types of batteries. A range of techniques for inducing TR was tested. The significant structural damage caused by a nail penetration experiment instantly causes a loss in acoustic signal due to the gaps appearing between layers and stopping acoustic transmission. Thermally-induced heating of the cell proved to be the most effective and reproducible method for inducing cell failure. The changes in ToF of the first echo peak correlate with cell temperature and give a clear indication of when a cell is heating. In these tests the electrolyte evaporation resulted in a loss of acoustic signal, providing a clear indication that significant cell heating and damage were occurring. To replicate more representatively real-world applications, the thermally induced TR experiments were repeated by heating only a small area of the cell. These tests showed that the technique could detect internal temperature changes long before the thermocouples placed on the surface of the cell. With the use of multiple transducers, it was also possible to detect the propagation of TR through a small module of cells. Indications that the cells were reaching dangerous temperatures were evident from acoustic measurements long before the first cell failed triggering a chain reaction through the pack and causing all cells to fail. Finally, acoustic measurements were proven to be particularly reliable, delivering consistent acoustic signals across different cells and significantly larger ToF changes than any observed in normal use in the case of abuse conditions.

From the results here presented, a short-term application could be to include ultrasonic monitoring as part of HORIBA MIRA's abuse testing approach to provide real-time access to internal states of the cell as well as more informative data and consultancy on test outcomes. With regards to onboard battery pack applications, while these results are very encouraging, there is a long way to go before "smart" batteries (i.e. containing an ultrasonic diagnostic system) can be commercially manufactured. To take the technology forward on the journey to mass-production, more comprehensive ultrasonic tests on a wide variety of batteries (encompassing the complete spectrum of battery types), looking across the complete range of operational variables (temperature, age, charging history, battery construction, etc) shall be performed. All tests will need to be repeated multiple times to statistically have confidence that the ultrasonic data can reliably show the condition of the battery. A cost-effective integrated ultrasonic transducer system including transducers, electrical connectivity, transducer drive electronics and signal analysis will need to be developed for each class of cell/battery.

Finally, an analysis needs to be made as to what proportion of cells within the battery pack needs to be monitored. A battery-analysis system that relied on a few cells within the pack being ultrasonically active would significantly reduce costs and greatly simplify the system connectivity. With this regard, a promising technique currently under investigation at UCL for monitoring electrochemical devices is acoustic emission. While the techniques discussed thus far rely on the generation of an ultrasonic pulse to probe the device and another, or the same transducer, to receive the altered acoustic signal, emission uses a single transducer to 'listen' for any sounds generated by the cell itself. In the typical setup used for an acoustic emission experiment, an acoustic emission sensor, effectively a transducer similar to those used for ultrasound testing, is placed on the cell of interest and sounds generated by the cell are monitored. This approach presents several advantages for battery pack

monitoring where it has the potential to sensibly reduce costs and system complexity.

Acknowledgments

The authors would like to acknowledge the European Automobile Manufacturers' Association (ACEA) for support in funding the experimental work here presented.

* Editorial note: This content is based on HORIBA's investigation at the year of issue unless otherwise stated.

References

[1] Q. Wang, B. Mao, S. I. Stoliarov, and J. Sun, "A review of lithium ion battery failure mechanisms and fire prevention strategies," Prog. Energy Combust. Sci., vol. 73, pp. 95-131, Jul. 2019.

[2] A. W. Golubkov et al., "Thermal runaway of commercial 18650 Li-ion batteries with LFP and NCA cathodes - Impact of state of charge and overcharge," RSC Adv., vol. 5, no. 70, pp. 57171-57186, 2015.

[3] Faiz Siddiqui, "A Tesla Model S erupted 'like a flamethrower.' It renewed old safety concerns about the trailblazing sedans," The Washington Post, 2020.

[4] Heekyong Yang, "Kona EV owners say Hyundai mishandling recall for battery fires," Reuters, 2020.

[5] James Edmondson, "China to Enforce Electric Vehicle Safety by 2021," 2020. [Online]. Available: https://www.idtechex.com/en/research- article/china-to-enforce-electric-vehicle-safety-by-2021/20707.

[6] M. Braglia, "Thermal Runaway and Thermal Propagation Detection," 2019.

[7] C. Mikolajczak, K. White, M. Kahn, and R. T. Long, Lithium-Ion Batteries Hazard and Use Assessment. SpringerBriefs in Fire, 2013.

[8] J. Garche and K. Brandt, Eds., Electrochemical Power Sources: Fundamentals, Systems, and Applications Li-Battery Safety. Elsevier, 2019.

[9] S. Koch, K. Birke, and R. Kuhn, "Fast Thermal Runaway Detection for Lithium-Ion Cells in Large Scale Traction Batteries," Batteries, vol. 4, no. 2, p. 16, 2018.

[10] X. Feng, C. Weng, M. Ouyang, and J. Sun, "Online internal short circuit detection for a large format lithium ion battery," Appl. Energy, vol. 161, pp. 168-180, 2016.

[11] C. Wu, C. Zhu, Y. Ge, and Y. Zhao, "A diagnosis approach for typical faults of lithium-ion battery based on extended Kalman filter," Int. J. Electrochem. Sci., vol. 11, no. 6, pp. 5289-5301, 2016.

[12] N. S. Spinner, C. T. Love, and S. G. Rose-Pehrsson, Susan L. Tuttle, "Expanding the Operational Limits of the Single-Point Impedance Diagnostic for Internal Temperature Monitoring of Lithium-ion Batteries," Electrochim. Acta, vol. 174, pp. 488-493, 2015.

[13] Z. Liao, S. Zhang, K. Li, G. Zhang, and T. G. Habetler, "A survey of methods for monitoring and detecting thermal runaway of lithium-ion batteries," J. Power Sources, vol. 436, no. June 2019, p. 226879, 2019.

[14] L. H. J. Raijmakers, D. L. Danilov, J. P. M. Van Lammeren, M. J. G. Lammers, and P. H. L. Notten, "Sensorless battery temperature measurements based on electrochemical impedance spectroscopy," J. Power Sources, vol. 247, pp. 539-544, 2014.

[15] L. H. J. Raijmakers, D. L. Danilov, J. P. M. Van Lammeren, T. J. G. Lammers, H. J. Bergveld, and P. H. L. Notten, "Non-Zero Intercept Frequency: An Accurate Method to Determine the Integral Temperature of Li-Ion Batteries," IEEE Trans. Ind. Electron., vol. 63, no. 5, pp. 3168- 3178, 2016.

[16] R. Srinivasan, P. A. Demirev, and B. G. Carkhuff, "Rapid monitoring of impedance phase shifts in lithium-ion batteries for hazard prevention," J. Power Sources, vol. 405, no. September, pp. 30-36, 2018.

[17] R. Srinivasan, B. G. Carkhuff, M. H. Butler, and A. C. Baisden, "Instantaneous measurement of the internal temperature in lithium-ion rechargeable cells," Electrochim. Acta, vol. 56, no. 17, pp. 6198-6204, 2011.

[18] B. G. Carkhuff, P. A. Demirev, and R. Srinivasan, "Impedance-Based Battery Management System for Safety Monitoring of Lithium-Ion Batteries," IEEE Trans. Ind. Electron., vol. 65, no. 8, pp. 6497-6504, 2018.

[19] R. Schwarz, K. Semmler, M. Wenger, V. R. H. Lorentz, and M. Marz, "Sensorless battery cell temperature estimation circuit for enhanced safety in battery systems," IECON 2015 - 41st Annu. Conf. IEEE Ind.

Electron. Soc., pp. 1536-1541, 2015.
[20] J. P. Schmidt, S. Arnold, A. Loges, D. Werner, T. Wetzel, and E. Ivers-Tiffée, "Measurement of the internal cell temperature via impedance : Evaluation and application of a new method," J. Power Sources, vol. 243, pp. 110-117, 2013.
[21] Y. S. Chou, N. Y. Hsu, K. T. Jeng, K. H. Chen, and S. C. Yen, "A novel ultrasonic velocity sensing approach to monitoring state of charge of vanadium redox flow battery," Appl. Energy, vol. 182, pp. 253-259, 2016.
[22] B. Sood, C. Hendricks, M. Osterman, and M. Pecht, "Health monitoring of lithium-ion batteries," Electron. Device Fail. Anal., vol. 16, no. 2, pp. 4-16, 2014.
[23] A. G. Hsieh et al., "Electrochemical-acoustic time of flight: In operando correlation of physical dynamics with battery charge and health," Energy Environ. Sci., vol. 8, no. 5, pp. 1569-1577, 2015.
[24] S. Bhadra, A. G. Hsieh, M. J. Wang, B. J. Hertzberg, and D. A. Steingart, "Anode Characterization in Zinc-Manganese Dioxide AA Alkaline Batteries Using Electrochemical-Acoustic Time-of-Flight Analysis," J. Electrochem. Soc., vol. 163, no. 6, pp. A1050-A1056, 2016.
[25] G. Davies et al., "State of Charge and State of Health Estimation Using Electrochemical Acoustic Time of Flight Analysis," J. Electrochem. Soc., vol. 164, no. 12, pp. A2746-A2755, Sep. 2017.
[26] L. Gold et al., "Probing lithium-ion batteries' state-of-charge using ultrasonic transmission - Concept and laboratory testing," J. Power Sources, vol. 343, pp. 536-544, 2017.
[27] P. Ladpli, F. Kopsaftopoulos, R. Nardari, and F.-K. Chang, "Battery charge and health state monitoring via ultrasonic guided-wave-based methods using built-in piezoelectric transducers," Smart Mater. Nondestruct. Eval. Energy Syst. 2017, vol. 10171, no. March, p. 1017108, 2017.
[28] Y. Wu, Y. Wang, W. K. C. Yung, and M. Pecht, "Ultrasonic Health Monitoring of Lithium-Ion Batteries," Electronics, vol. 8, no. 7, p. 751, 2019.
[29] J. B. Robinson et al., "Identifying Defects in Li-Ion Cells Using Ultrasound Acoustic Measurements," J. Electrochem. Soc., vol. 167, no. 9626352, 2020.
[30] R. E. Owen et al., "Operando Ultrasonic Monitoring of Lithium-Ion Battery Temperature and Behaviour at Different Cycling Rates and under Drive Cycle Conditions," J. Electrochem. Soc., vol. 169, 2022.

Michele Braglia
ミシェル ブラグリア
Energy Systems Innovation Lead
Mobility Innovation Hub
HORIBA MIRA

Richard Stocker
リチャード ストッカー
Principal Engineer (Battery Solutions)
HORIBA US,
Mobility Innovation Hub
HORIBA MIRA